Proceedings of the CAS–CERN Accelerator School: Beam Injection, Extraction and Transfer, Erice, Italy, 10-19 March 2017, edited by B. Holzer, CERN Yellow Reports: School Proceedings, Vol. 5/2018, CERN-2018-008-SP (CERN, Geneva, 2018)

Exotic Injection and Extraction Methods

B. Goddard
CERN, Geneva, Switzerland

Abstract
This paper is intended to give a flavour of the creativity that can be applied to injection and extraction, in terms of concepts, systems, challenges, and solutions that are somewhat unconventional. A dazzling array of techniques and technologies were already described in great detail in the other papers; 'conventional' is, therefore, a very relative or subjective term. In this paper, some of the more unusual or creative methods for filling or emptying accelerators are presented and discussed.

Keywords
CAS; injection; extraction; kickers; septa; losses, emittance; laser; muons.

1 Introduction

The domain of beam transfer lends itself to the development of creative solutions to the problems and constraints that are particular to the processes of injecting and extracting particles from accelerators. An array of fantastic beasts were already described in the CAS course—some of the topics already seen include:

- electrostatic spiral inflectors for cyclotrons;
- golf-club longitudinal injection for small-aperture storage rings;
- multipole kicker for light-source top-up injection;
- corkscrew gantry for medical hadron beam delivery;
- slip-stacking and phase-space painting;
- magnetic splitting.

Given the richness already present in the mainstream techniques, in widespread use and based on standard systems, it is justifiable to wonder why even more exotic methods are required. Some of the rationale is to make possible what would otherwise be inaccessible, where no conventional solution exists. In addition, in the real, imperfect world, many limitations are present, which arise from the laws of physics, engineering limits, safety constraints, economic imperatives, etc. Specific factors that come into this category of limitation are beam stability, lifetime of unstable particles, physical space available, maximum electric or magnetic field, beam loss, and radiation dose.

Sometimes the progress is driven by the imagination of the accelerator builders—the new ideas are so elegant that they allow accelerators to move into new regimes of accelerator performance.

In this paper, the exotic technologies and methods described are a massless septum for extraction or for injection failure mitigation, an open C-core extraction kicker, injection into a muon decay ring, extraction with bent crystals, and laser stripping H^- injection. There are many, many other fascinating topics in the field, illustrating the interplay between hardware, technology, and accelerator physics—students are encouraged to explore the available literature, some of which is listed in the references section.

2 Massless septum

To an accelerator physicist charged with designing an injection or extraction system, a massless septum sounds very exciting. Ideally, as for any septum, a narrow septum width is desirable. The rather large

https://doi.org/10.23730/CYRSP-2018-005.553

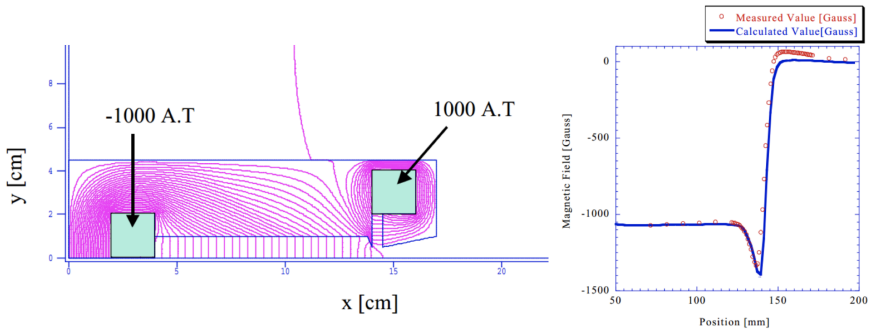

Fig. 1: Cross-section and field in septum region for a basic massless septum design

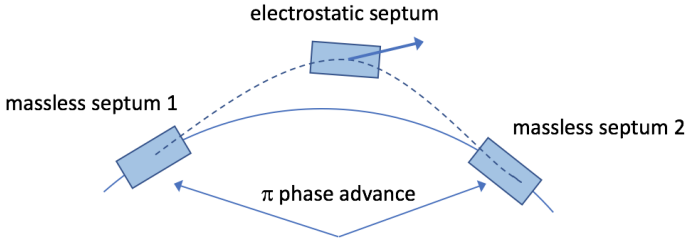

Fig. 2: Massless septum deployment for multiturn extraction loss reduction

practically attainable septum thickness constrains its use to a subset of applications, but the device remains a fascinating technological concept. The relatively thick 'septum' width is of the order of the gap height (Fig. 1)—this pushes its useful application domain to higher beam energies or electron beams, where small gaps are possible for the tiny physical emittances, or to low beam energies, where large bending angles can be achieved to clear the septum width.

The most attractive potential applications are those difficult systems for injection and extraction processes where beam interception at the septum blade is problematic, for example to reduce beam loss in slow or continuous extraction over many turns, or to prevent damage from mis-steered beams in injection or extraction systems of high-energy machines.

The massless septum has been deployed in several accelerators. For the 150 MeV Kyoto FFAG [1], a massless septum was used to extract a high-power CW beam with low losses, a concept which was has also been studied for other similar high-power machines. For the Kyoto FFAG, the massless septum was deployed as a closed bump around the electrostatic septum (ES), which allowed a large reduction in the density of particles impacting the ES. The FFAG is a hybrid of cyclotron and synchrotron, with quasi-continuous high current and adjacent turns that are very close together—requiring a thin septum to minimize extraction losses. A pair of massless septa can reduce the beam losses on the septum, as illustrated schematically in Fig. 2.

A version of this concept has also been explored in more detail in potential application to ES beam-loss reduction of a conventional synchrotron slow extraction [2]. The beam distribution is 'stretched' by a massless septum at $\pi/2$ phase advance upstream of the ES to reduce density. The septum width (where the field increases from zero to its nominal value) is crucial in the achievable loss reduction (Fig. 3). Only a single massless septum is required, but the disadvantage with this arrangement is that a large physical anode–cathode gap is needed for the ES to accommodate the normal and stretched part of the spiral step, which would limit the attainable ES field.

This limitation could be improved by shifting the ES position outwards to cut the stretched part of the distribution at the other end, with the perturbation closed by a second massless septum a further $\pi/2$

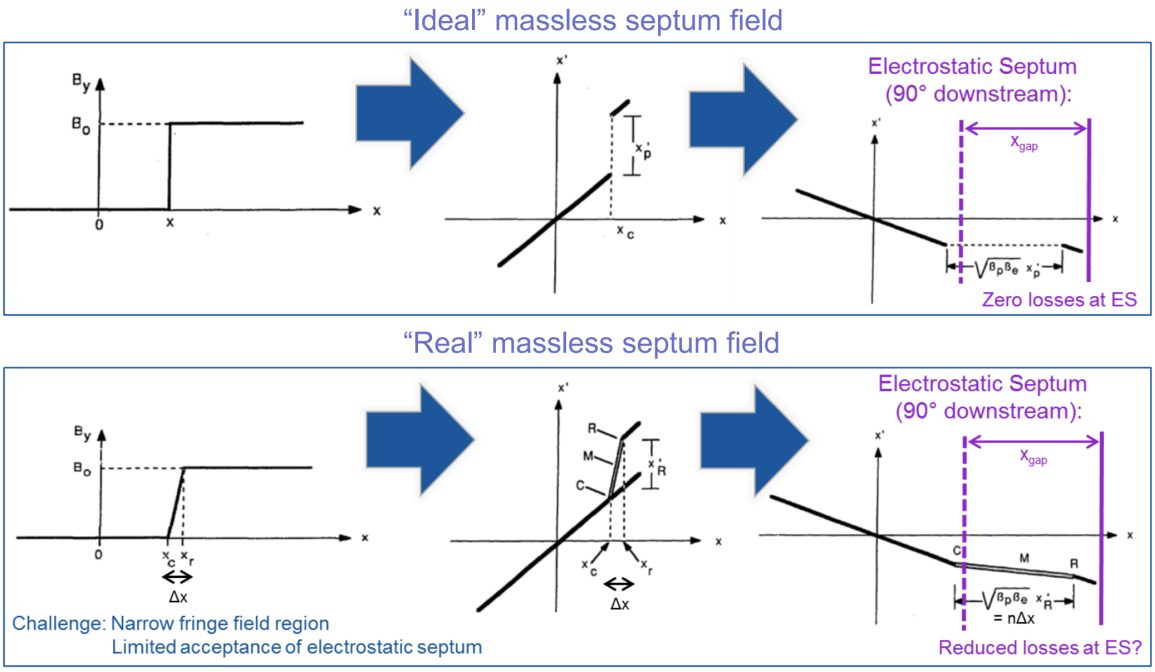

Fig. 3: Phase-space representation of massless septum used to reduce particle density at the electrostatic septum. Top: the case with a perfect zero-width septum. Bottom: a more realistic field distribution.

downstream. This maintains the separatrix size inside the ES gap, but requires a larger circulating beam aperture between the massless septa to accommodate the stretched separatrix. This scheme is illustrated in Fig. 4.

The massless septum concept has also been investigated for low-energy beam transport, for example, in the accelerator-driven neutron source FRANZ [3]. The low-energy proton beam at 120 keV, 50 mA, needs to be transported with very low losses. A novel massless septum system has been designed after the chopper for the beam separation to the dump (Fig. 5), which consists of a C-magnet with optimized pole shapes, which will extract the beam with minimal losses, and a magnetic tube to shield the beam from the fringe field of the dipole.

3 Open C-core kicker

It can be difficult to define extraction kicker magnets for high-energy beams, owing to conflicting constraints. One the one hand, high kick strength is always preferable, together with fast rise time, and high beam energy means a lot of $\int B.\mathrm{d}l$, which pushes the system towards small gaps in the non-kicked plane, high current, and long magnetic length. On the other hand, beam coupling impedance is often a performance concern, and this pushes the system towards larger gaps, shorter installed length, and shielding of ferrites, which can increase the gap and rise time.

Crucially, for a proton or ion accelerator, the beam at injection energy is generally significantly physically larger than at extraction, owing to the conservation of the normalized transverse emittance. A conventional full-aperture extraction kicker must be large enough to accept the injected beam. For large energy swings, this can mean a lot of 'wasted' aperture, as the physical beam size scales with $(\beta\gamma)^{0.5}$, plus some extra millimetres of aperture for injection oscillations. An interesting kicker concept is based on this fact, since the kick strength is only needed at the extraction energy, where the beam is small. The concept uses an open C-type kicker with a small vertical gap (Fig. 6), and a fast bumper system to move the beam into the kicker gap shortly before extraction, where it would remain for only a few tens

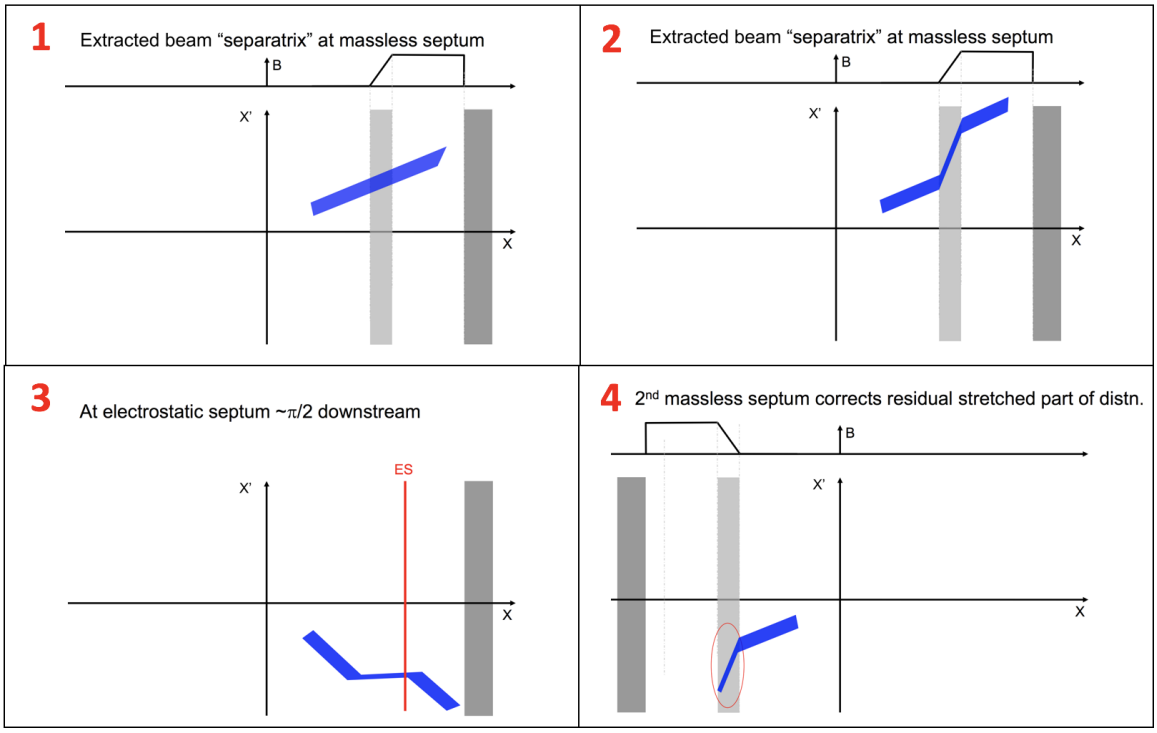

Fig. 4: Pair of massless septa used to reduce particle density at electrostatic septum, with the second septum refolding the separatrix back.

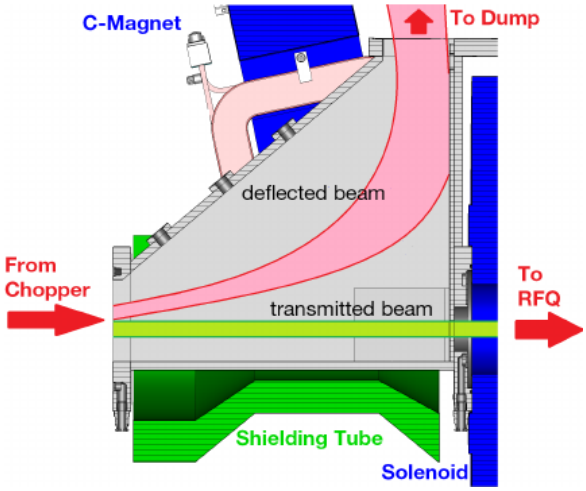

Fig. 5: Massless septum for 120 MeV proton beam separation for FRANZ chopper system

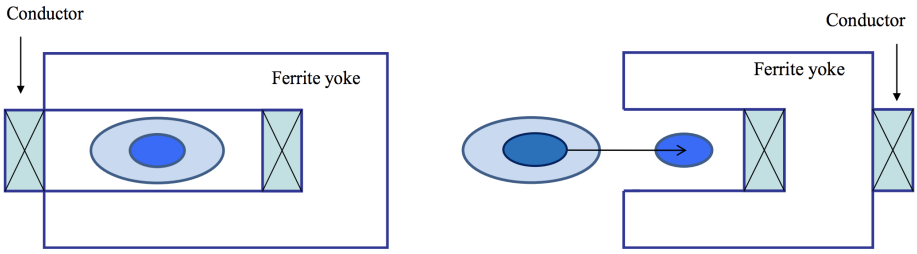

Fig. 6: Full-aperture (left) and open C-core (right) extraction kicker cross-section, where a fast bump is used to move the beam into the gap. The vertical gap height is determined by the injected beam size for the full-aperture system, and by the extracted beam size for the open C-core system.

of milliseconds.

Having the beams present in the kicker gap for a short time only, and then at high energy, would be a big advantage with respect to beam stability arising from the kicker beam coupling impedance. Similarly, kicker heating from the real part of the beam coupling impedance will be much less of an issue if the high coupling impedance seen by the beam is only seen for a very short time, resulting in a very small averaged power deposition. In addition, since a smaller vertical gap is required (for a given current), a shorter installed kicker length will be required, which helps reduce the overall beam coupling impedance. Overall, the kicker system can be much more compact, at the cost of needing an extra closed orbit bumper system. This concept has actually been used for the AGS beam extraction system at BNL [4].

4 Stochastic muon decay ring injection

Intense circulating muon beams are of great interest as a controlled source of neutrinos for, e.g., light sterile neutrino searches or precise cross-section measurements. Muons are unstable leptons with negative or positive charge (antimuons), 200 times the electron mass and a lifetime at rest of 2.2 µs. The muon decays into an electron, an electron anti-neutrino, and a muon neutrino:

$$\begin{aligned} \mu^- &\to \mathrm{e}^- + \overline{\nu}_\mathrm{e} + \nu_\mu \,, \\ \mu^+ &\to \mathrm{e}^+ + \nu_\mathrm{e} + \overline{\nu}_\mu \,. \end{aligned} \tag{1}$$

One concept to store muons proposes a 400 m circumference racetrack decay ring filled with muons [5], to produce intense neutrino beams. The muon lifetime is about 60 turns in the ring. The ring would be oriented such that the neutrinos produced from the decay straight are directed towards a detector, Fig. 7. The beam from the decay straight is preferred for the experiment, as it is uncontaminated by muon anti-neutrinos (for the case of a μ^- ring).

The muons are produced from decay of $\sim$5 GeV/c pions (themselves composed of an up and down quark–antiquark pair with a lifetime at rest of only 26 ns). The pions are produced from directing a high-power 10–100 GeV proton beam on a target. The injection system uses the fact that the 5 GeV/c pions decay to muons with very different momenta—a wide distribution centred on 3.8 GeV/c and ranging from about half the pion energy to almost the full energy. The ring optics and injection layout merges pions and already-circulating muons in a special dipole, to 'defeat' Liouville (a victory that is the ambition of every injection system designer). The injection straight needs to be long, to allow as many pions as possible to decay, with optics that are simultaneously matched for the two very different particle momenta, and the ring needs a huge momentum acceptance to be able to store the resulting muons.

This is shown schematically in Fig. 8. Note that only about 50% of the pions decay in the injection straight and, as they will not be transmitted through the acceptance of the downstream arc, an extraction

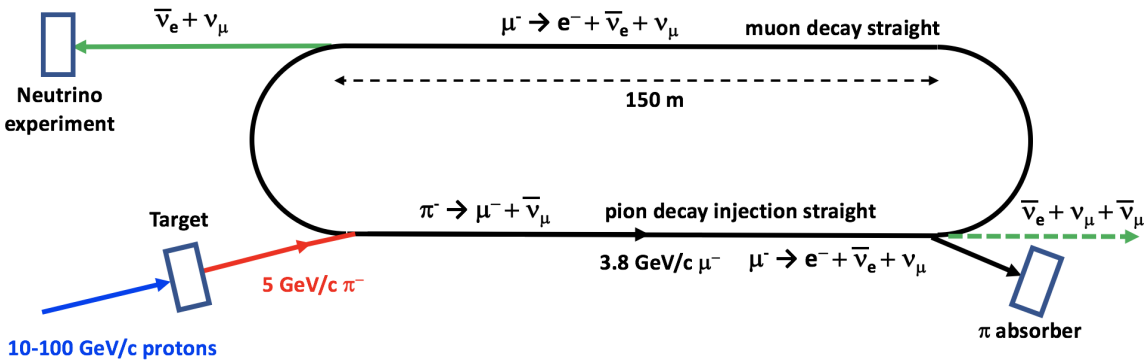

Fig. 7: Concept of muon storage ring to produce high-intensity neutrino beam

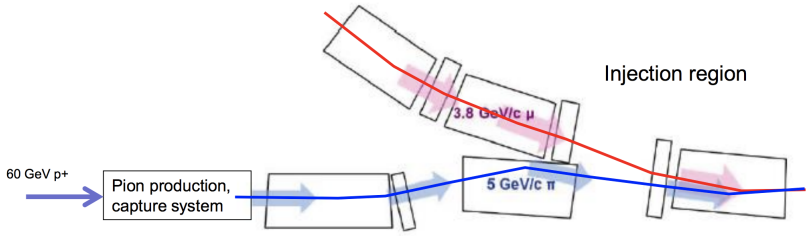

Fig. 8: Stochastic injection of pions in muon storage ring. Pions and muons of very different momenta are merged in the injection dipole.

(separation) dipole and absorber are needed at the end of the straight, essentially a reverse of the injection system. The ring acceptance needs to be about $\pm 10\%$, which is extremely large compared with most accelerators ($\sim \pm 0.1\%$ is more typical).

5 Extraction with bent crystals

In addition to the usual magnetic or electrostatic elements, charged particles can also be deflected by a bent crystal, see e.g., Ref. [6]. The potential wells between the atomic planes confine particles with small enough transverse momentum (Fig. 9); if the crystal is bent with an angle small enough to maintain the confinement, the particles can be bent though the same angle, in a very short longitudinal distance. These confined particles are said to be *channelled*; other distinct effects have been identified in the coherent and incoherent scattering behaviour, as elucidated in Ref. [7]. Channelling gives the biggest deflection, while volume reflection results in the highest efficiency.

Bent crystals are already deployed in high-energy proton accelerators, including heavy-ion collimators for the LHC [8]. One other very interesting potential application is slow extraction of multi-teraelectronvolt protons [9]. Producing a slow-extracted beam from the LHC at 7 TeV or from FCC at 50 TeV will be very challenging, as it is more and more difficult to design a conventional slow extraction system as the beam energy reaches the teraelectronvolt regime, with superconducting rings. A large machine aperture is needed for 1/3 integer resonance, superconducting magnets are very sensitive to beam losses, and the technological limit of $\sim$10 MV/m for electrostatic septa coupled with the extreme beam rigidity means that the length of extraction systems simply becomes unfeasibly large. For example, for FCC the $B\rho$ at 50 TeV is a huge 166,000 Tm. Around 500 m of ES field length would be needed to produce a deflection of the order of 0.1 mrad, which would be almost impossible to accommodate in a

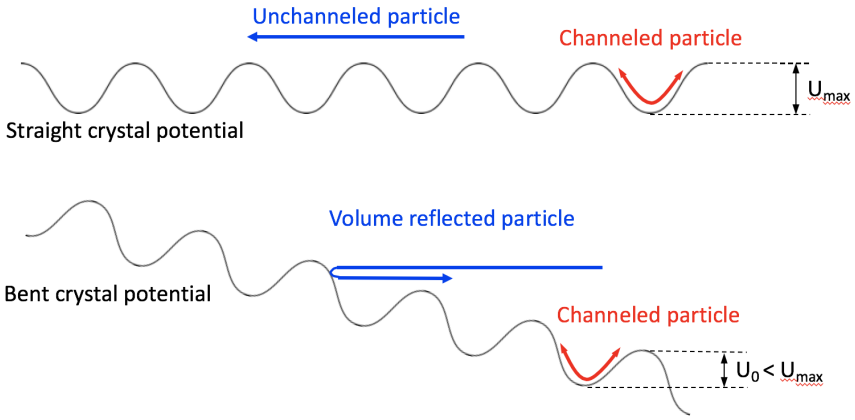

Fig. 9: Potential distribution for straight (top) and bent (bottom) crystal. The channelling probability for an impacting proton depends critically on the transverse momentum, which must be less than the potential well height. Bending the crystal introduces an asymmetry into the potential well (bottom), which reduces the channelling probability.

lattice, or to align in practice, given that the septum is a thin element of <0.1 mm thickness.

A bent crystal with a bending radius R channels a beam of energy pv if $pv/R \simeq 1$ GeV/cm. A condition can be derived for the maximum angle θ_c that can be accepted:

$$\theta_c \leq \sqrt{\frac{2U_{\max}}{pv}} \,. \tag{2}$$

This is simply astounding—taking 7 TeV protons, this gives $R \simeq 70$ m. For comparison, the 8 T LHC dipoles bend the 7 TeV protons with $R \approx 3000$ m. So the bent crystal is as effective as a 330 T magnet. A 2 cm length of bent crystal can deflect 7 TeV protons by 0.3 mrad, which is more than enough to act as the first element in an extraction system. Bent crystals, therefore, may have the potential to replace huge 5–500 m long ES devices needed at 100 GeV to 50 TeV energies, with extremely compact millimetre- or centimetre-long devices.

In addition to the possible application for collimation and extraction elements, crystals have also been proposed [10] as a way to reduce beam loss on a thin ES for conventional slow extraction. If the crystal alignment and position can be maintained through the spill in such a way as to ensure channelling, the low-loss coherent deflection of protons impacting the crystal can be used to shadow the ES and reduce by a large factor the number of particles impacting the ES (Fig. 10).

6 Laser stripping for H^- injection

The H^- ion is a fantastic ion for accelerators. It is charged, so can be accelerated and deflected; it is easy to produce and stable (the e^- binding energies are 0.75 and 13.6 eV); and the weakly-bound e^- can easily be removed with thin foil, allowing the astute designer to 'defeat Liouville' by injecting on top of an existing distribution. However, the interaction processes in the physical stripping foil means that beam loss, foil heating, or damage (Fig. 11), and unwanted emittance growth can all occur. These problems are especially acute in high-energy, high-power machines, such as SNS [11].

Before entering into the details of the laser stripping process, an aside into the dynamics of the H^- ion is needed. An H^- ion passing through a transverse magnetic field B with velocity βc experiences an electric field E in its own rest frame:

$$E = \beta\gamma c \times B \,. \tag{3}$$

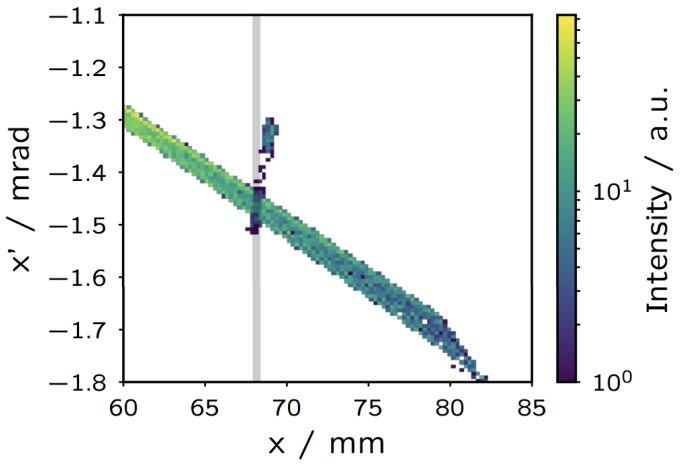

Fig. 10: Transverse phase-space distribution of 1/3 integer slow extraction separatrix at ES location, after coherent channelling by an upstream bent crystal. A reduction in particle density at the ES (vertical line) is clearly visible.

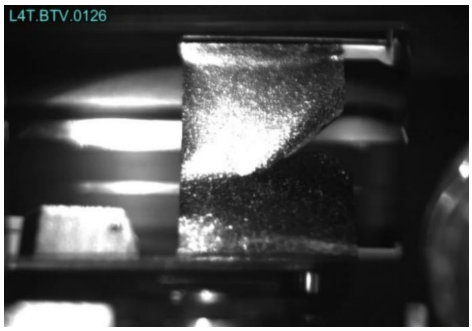

Fig. 11: Damaged carbon stripping foil of the CERN PS booster 160 MeV H^- injection system

This electric field can be strong enough to remove the loosely bound outer electron, which only has a 0.75 eV binding energy. This field stripping (or Lorentz stripping) can lead to uncontrolled beam loss. The effect worsens with increasing beam energy, compounded by the (usual) increase in magnetic field for accelerator elements at higher energy. The fractional beam-loss rate per metre of field can be derived as:

$$\frac{\mathrm{d}F}{\mathrm{d}S} = \frac{B}{A_1} \exp\left(-\frac{A_2}{\beta\gamma cB}\right), \tag{4}$$

where A_1 and A_2 are constants with numerical values 2.47×10^{-6} V s/m and 4.49×10^9 V/m.

Normally, radio-protection considerations limit beam loss to something like 0.11 W/m of beam-loss power, which places a practical upper bound on the maximum allowable magnetic field, which depends very strongly on beam energy. This becomes an issue for injection and transfer line (dipoles, quadrupoles, correctors) at H^- beam energies at or above the 1 GeV level. But this unique effect of Lorentz stripping provides a great opportunity for the creative thinking that has gone into the laser stripping concepts. U The basis for laser stripping is the observation that excited neutral H^0 is easy to field strip in a magnetic field, with the lifetime as a function of field depending on the principle quantum number n of the excited state (Fig. 12). For instance, at 1 GeV, both the ground-state H^- and H^0 in the $n = 3$ excited state are easy to Lorentz strip with a 1–2 T magnetic field. The lifetime is between 10^{-10} and 10^{-9} s, which with $v \simeq c$ means that the electron is removed within a few tens of centimetres of field.

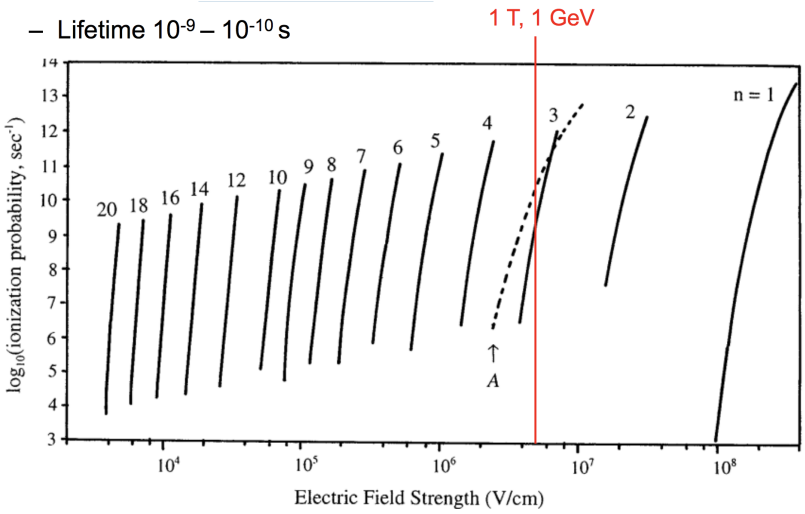

Fig. 12: Ionization probability vs. electric field for different H^0 principle quantum numbers. The electric field associated with a 1 GeV proton in a 1 T field is shown as the red vertical line.

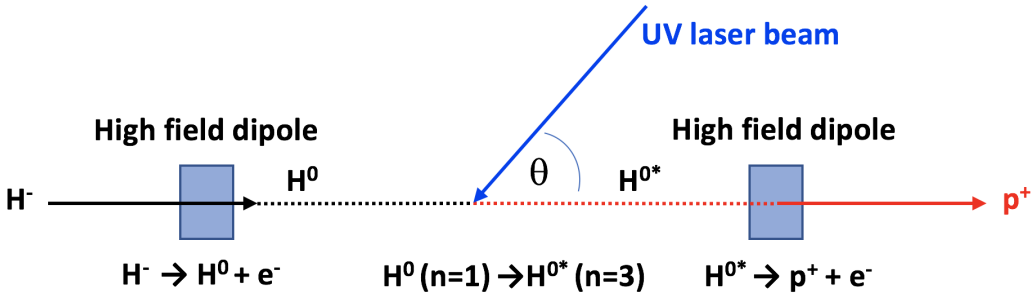

Fig. 13: Three-stage laser stripping scheme, relying on two field-stripping stages with an intermediate resonant excitation of the H^0.

A basic laser stripping scheme [12] is illustrated in Fig. 13. In fact, the laser does *not* strip either electron directly. There are three distinct steps.

1. Removal of loosely bound e^- from H^- with strong magnet ($\sim$2 T). This is in the vertical plane to avoid increasing spread in horizontal angles x'.
2. Resonant excitation of second e^- to high energy level: $n = 1$ to $n = 3$ (or higher) transition, using a high-power tuned laser.
3. Removal of excited electron with another strong magnet ($\sim$2 T).

The injection needs to be accommodated in the real machine layout, and also provide the normal advantages of the H^- injection in terms of phase-space painting over many turns. A schematic layout of an injection system designed for 4 GeV H^- injection with laser stripping is shown in Fig. 14 [13].

The key to the laser stripping is resonant laser excitation of the neutral H^0 ion. Here the hydrogen energy level diagram, Fig. 15, is revealing. For 1 GeV H^-, at least the $n = 3$ level needs to be reached, which requires absorption of a 12.1 eV photon. This is very far into the ultraviolet, at 103 nm, and difficult to produce with the required high laser intensity. But here nature comes to the rescue with a rare example of a free lunch—the relativistic Doppler shift modifies the frequency f_s of the photon in the

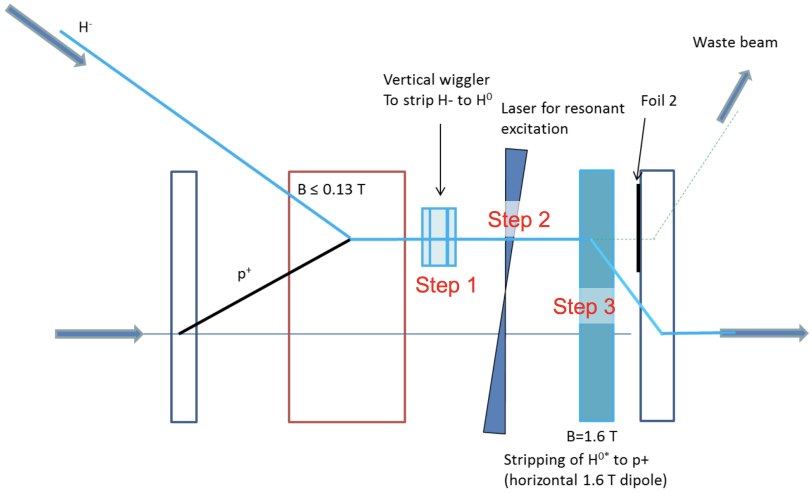

Fig. 14: Injection system designed for 4 GeV H^- injection with laser stripping

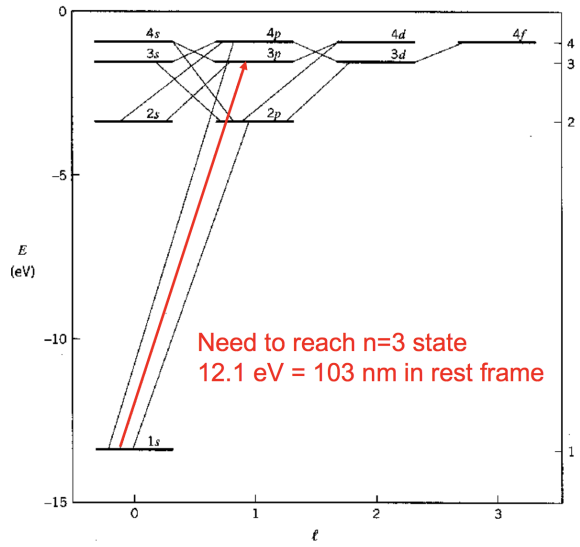

Fig. 15: Neutral hydrogen energy level diagram, including fine-structure splitting

frame of the ion, according to the relativistic parameters and the incident angle θ_0, according to

$$f_s = f_0\gamma(1 + \beta\cos(\theta_0)) \,. \tag{5}$$

For angles approaching head-on, and for high beam energies, this enhancement factor approaches 2γ, so for a 1 GeV proton the resonance to excite the $n = 3$ state can be achieved with 355 nm photons interacting with an angle of about 40° to the protons. This opens another very attractive feature, which is the ability to tune the effective resonant laser frequency by adjusting the interaction angle, allowing the use of standard laser wavelengths for high-power systems, e.g., 532 or 355 nm.

The devil, as always, is in the details, and one of the most difficult problems is the laser power required to saturate the resonance transition. There are several intricate details worthy of explanation, which beautifully illustrate the inventiveness and ingenuity of those who have evolved this concept.

The first problem is to excite all the neutral ions to the higher quantum state. For a two-state quantum system, this can be neatly achieved by adiabatic rapid passage, where the exciting frequency is

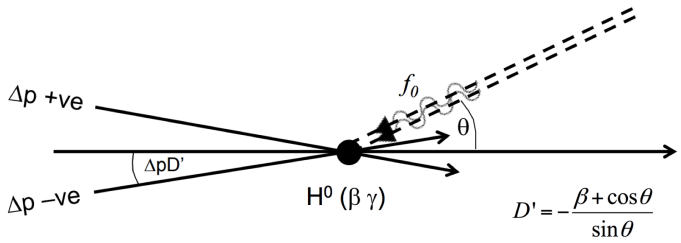

Fig. 16: Dispersion tailoring to cancel Doppler shift at interaction point for laser stripping resonant excitation step, by correlating particle momentum with interaction angle.

swept across the transition frequency, which, for a suitable choice of parameters, ensures that 100% of the population finishes in the upper state. Sweeping the laser frequency is deeply unattractive, but again nature provides a way out, in the angular dependence of the Doppler shift given in Eq. 5. The correct conditions can be arranged by making the laser beam slightly divergent at the interaction region, as the change in θ is seen by the beam as a change in frequency. Only a very small beam divergence, of the order of microradians, is needed to to cover the narrow resonance linewidth.

A more difficult problem is presented by the spread in particle momenta and angles, which means that each individual particle has a different resonant frequency. This is effectively a Doppler spread, as encountered in conventional spectroscopy. The spread in particle angles from the beam emittance and lattice is typically 10^{-4} to 10^{-5} with small α, large β and normalized emittance of the order of micrometres. The beam momentum spread $\Delta p/p_0$ is typically 10^{-3} to 10^{-4}, and these effects change the resonant frequency by the same amount. These are much larger than the laser frequency spread or the resonance linewidth; increasing the laser frequency spread would require a large increase in the overall required laser power, which is technically very difficult.

To overcome the Doppler spread, it is possible to further increase laser divergence at the interaction point to the order of a milliradian, such that the resulting frequency spread then covers the Doppler spread from Δp. This solves the technical issue associated with spreading the laser frequency, but only a small fraction of the available laser photons are actually in resonance with the transition, which again requires more laser power.

A more elegant way to overcome Doppler broadening is to arrange a correlation between the individual particle momentum offset and the interaction angle θ. This can be achieved by dispersion tailoring: arranging the dispersion angle D' at the IP such that a change in angle of the individual particle generated by its momentum offset matches the difference in frequency of the resonance arising from this offset. This is illustrated schematically in Fig. 16. It is simple to show that the required D' is given by

$$D' = -\frac{\beta + \cos(\theta)}{\sin(\theta)} \,. \tag{6}$$

The final part of the laser stripping process is the removal of the excited second electron. In the SNS experiment, this is done by stripping in the fringe field of the chicane dipole. The lifetime of the excited ion depends on both the energy level and the magnetic field. Since the stripped particle is then deflected in the remainder of the magnetic field, stripping at a different S position gives a different deflection angle, and hence an emittance increase. This can be acceptable for beams with large emittance, but could be an issue for very bright beams. The stripping dipole field should be as 'hard-edged' as possible, to minimize the stripping length, but another complication comes from the different stripping rates associated with the fine and hyperfine structure in the excited ion energy levels. This effect is illustrated in Fig. 17 [14], where the fraction of unstripped beam remaining for the different excited states is plotted as a function of position in the stripping dipole field. The advantage of a high-lying excited state is clearly apparent.

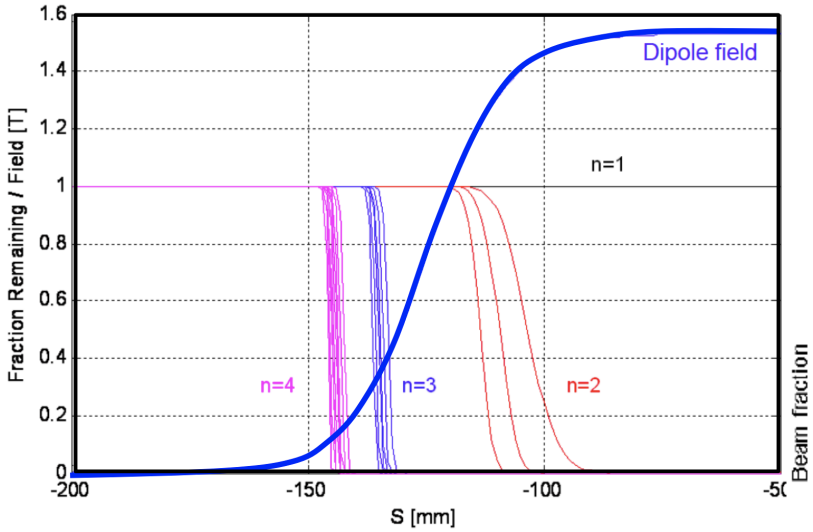

Fig. 17: Stripping of excited 4 GeV H^0 in a 1.5 T dipole fringe field. The multiple curves for each principle excited state are due to the fine and hyperfine structures.

The main performance limitation is the laser power to reach a high efficiency, given by:

$$P_{\text{peak}} = \frac{\ln(1/\delta)\hbar^2\epsilon_0 c^2 \kappa\omega_0\tau_1 \sin\theta h}{2\mu_{1n}^2\gamma(1+\beta\cos\theta)^2}\,, \tag{7}$$

where $\delta \ll 1$ is the ratio of unexcited to excited atoms, $2h$ the vertical beam size, ω the laser frequency in the laboratory frame, $\kappa = 6\Delta\lambda/\lambda$ the full relative frequency change, τ_1 the laser micropulse duration and μ_{1n} the Einstein dipole transition coefficient. For the SNS injection at 1 GeV, this turns out to be about 10 MW peak power, which is obviously not feasible in any quasi-CW way. Many ingenious proposals are combined to reduce the average laser power to a technically feasible level:

- dispersion tailoring to reduce Doppler spread: 10 MW $\rightarrow$ 2 MW;
- reduce vertical beam size and α_x: 2 MW $\rightarrow$ 1 MW;
- match laser macro-pulse to H^- beam duty factor: 1 MW $\rightarrow$ 20 kW;
- mode-lock laser pulses to 30 ps at 402 MHz: 20 kW $\rightarrow$ 240 W;
- $\times$50 recycling of laser power in Fabry–Pérot cavity: 240 W $\rightarrow$ 5 W.

7 Conclusion

The examples presented in this paper illustrate that beam transfer offers some unique opportunities for merging different domains of physics, engineering, and technology. The next breakthrough may come from a totally a different domain, as evidenced by the overlap already with solid-state physics and quantum optics.

There is always scope for creativity and elegance in the design of these systems. It is crucial to stay in touch with other disciplines, and to use imagination in approaching new (and indeed old) problems.

8 Acknowledgement

Thanks are due to the many colleagues who contributing knowingly or unknowingly to the topics described herein, and for their great creativity in tackling difficult problems in beam transfer.

References

[1] Y. Yonemura *et al.*, Beam extraction of the PoP FFAG with a massless septum, Proc. PAC, 2003.

[2] M. Barnes and B. Goddard, Considerations on a new fast extraction kicker concept for SPS, sLHC Project Note 0018, (CERN, Geneva, 2010).

[3] C. Wiessner *et al.*, Massless beam separation system for intense ion beams, Proc. PAC, 2015.

[4] W.T. Weng *et al*., The AGS fast kicker magnet systems, Part. Accel. Conf., Washington, DC, 1981.

[5] D. Neuffer, *IEEE Trans. Nucl. Sci.* **NS-28**, (1981) 2034, https://doi.org/10.1109/TNS.1981.4331584.

[6] E.N. Tsyganov, Preprint TM-682, TM-684, Fermilab, Batavia (1976).

[7] W. Scandale *et al.*, High-efficiency volume reflection of an ultrarelativistic proton beam with a bent silicon crystal, PRL 98, 154801 (2007), https://doi.org/10.1103/PhysRevLett.98.154801.

[8] D. Mirachi, Crystal collimation for LHC, CERN-ACC-2015-0143, (CERN, Geneva, 2015).

[9] W. Scandale *et al.*, *Nucl. Instrum. Methods Phys. Res. B* **355** (2015) 390, https://doi.org/10.1016/j.nimb.2015.01.043.

[10] F. Velotti, Reduction of resonant slow extraction losses with shadowing of septum wires by a bent crystal, Proc. IPAC, 2017, p. MOPIK050.

[11] J. Wei *et al.*, Evolution of the spallation neutron source ring lattice, Proc. 20th ICFA Advanced Beam Dynamics Workshop, Chicago IL, 2002, https://doi.org/10.1063/1.1522612.

[12] V. Danilov *et al.*, *Phys. Rev. ST Accel. Beams* **6** (2003) 053501, https://doi.org/10.1103/PhysRevSTAB.6.053501.

[13] W. Bartmann *et al.*, A doublet-based injection-extraction straight for PS2, Proc. IPAC'10, Kyoto, 2010, p. 3945.

[14] B. Goddard *et al.*, Laser stripping for the PS2 charge-exchange injection system, Proc. IPAC'09, Vancouver, 2009, p. TU6RFP028.